Journal of Harbin Engineering University
ISSN: 1006-7043

Vol 45 No. 6
June 2024

Flexural Performance of GPC one-way Slabs Reinforced with GFRP Reinforcements

Sai Kumar.A[1*], Kumaran.G[2]

[1] Ph.D Scholar, Department of Civil and structural Engineering Annamalai University, Chidambaram, India

[2] Professor, Department of Civil and structural Engineering, Annamalai University, Chidambaram, India

Abstract

This paper presents the flexural characteristics of Binary GeoPolymer concrete (GPC) one-way slabs reinforced with GFRP(Glass Fibre Reinforced Polymer) rebars under Laboratory two point Static loading condition. Generally GPC is a combination of Flyash as a main binder constituent and other source materials namely Ground Granulated Blast furnace(GGBS), Rice Ash , Alcofine etc.. In this study 70% Flyash combined with 30% GGBS is used instead of Ordinary Portland Cement to produce greenery material as well as to reduce the emission of Carbondioxide during Cement Production. Investigations were piloted on GPC one way slabs subjected to four point bending test experimentally. Totally five slabs were considered with different parameters for the analysis such as load and deflection characteristics along with ultimate load capability.

Keywords: Flexural behaviour, Fly Ash, GeoPolymer concrete, GFRP reinforcements, load-deflection characteristics

1. Introduction

One of the industries with the fastest global growth is construction. Current global figures indicate that around 260,00,00,000 tons of cement are needed annually. In the following ten years, this amount will rise by a quarter. Since limestone is the primary raw material used to make regular Portland cement, a severe scarcity of the material could develop after 25 to 50 years. Furthermore, a ton of carbon dioxide, a serious threat to the environment, is released into the atmosphere during the production of one ton of cement. Cement production also requires a massive amount of energy in addition to the already mentioned. Finding a substitute binder is therefore crucial.

GPC is the most technologically forward-looking material. Davidovits first proposed the idea of Geo polymer concrete in 1974. Essentially, it was cement replaced with industrial waste. Flyash, a waste product of the thermal industry, is just thrown onto the ground and takes up a lot of space. By creating Geopolymer Concrete, all of the aforementioned problems can be rearranged and resolved due to the fact, GPC doesn't require cement, which will limit atmospheric pollution from carbon dioxide emissions. The most advantages are sophisticated tensile and compressive strength, less shrinkage, and improved resistance to temperature along with chemical bout. Fly ash, GGBS, rice husk ash, and other industrial by-products are combined with an alkali solution to make GPC. Source materials, concentration of alkali, and conditions of curing evolutes the polymerization process and in turn contributes strength to GPC. All fly ash, with the exception of ASTM Class C fly ash, which has a high calcium concentration, is not binding at the same time. Pozzolanic activity occurs when fly ash is replaced partially or added as an admixture to OPC. The behaviour of OPC beams in combination with FRP bars under static stress has been the subject of numerous investigations carried out in recent years [1–20]. Few studies have been done, yet, to examine the GPC beams' capacity with FRP bars.

2. Literature Review

A vast study of literatures on GPC was done, with a focus on the combinations of fly ash with GGBS. The primary focus is on identifying the research gaps related to GPC development and expanding the understanding of the various strategies for supporting environmentally conscious GPC. Consequently, a concise review of the literature on the experimental study of GPC has been prepared.

In 2012, Naidu et al. examined the strongest characteristics of GPC made in five different ratios with minimal fly ash and slag content. According to reports, the formulation with a higher GGBS concentration has a high compressive strength at just 14 days—nearly 90% of its total compressive strength. Maranan et al. employed four-point bending tests to explore the reinforcement and anchorage systems effects.It has been observed that the diameter of the GFRP bars had no noticeable effect on the flexural performance of the tested beams but enhances the serviceability enactment of the beams.

Using GGBS and crusher sand, Patel et al. (2013) tested the behaviour of high performance concrete. Ahmed et al. [35] looked at the impact of different types of concrete, compressive behaviour and reinforcement ratio on the behaviour of GPC beams reinforced with carbon-Fibe Reinforced Polymer (CFRP) bars.

Supraja and Rao (2016) investigated the GGBS material when it completely substitutes Portland cement and the products are bound with sodium hydroxide and silicate, two alkaline liquids. The authors took into account sodium hydroxide solutions with molarities of 3M, 5M, 7M, and 9M. It was discovered that when the molarity of sodium hydroxide increases, so does the intensity of the Geopolymer. Under ambient temperature settings, Kathirvel et al. (2013) assessed the impact of various GGBS ratios (0-100%) on fly ash-oriented GPC. It was looked into how the amount of alkaline activated solution in the GPC mixture affected compressive strength.

Additionally, Cui et al. conducted experiments and statistical analyses to investigate the mechanical properties of geopolymer concretes in 2020.According to the findings of Maranan et al. (2015), the sand coating that was applied to the surface of the GFRP bars provided enough mechanical interlock and friction force resistance to guarantee a composite action between the bars and the GPC. Because of the GFRP bars' lower elastic modulus, concrete beams reinforced with them have less post-cracking flexural stiffness than beams normally reinforced with steel bars (Ascione et al. 2010). The authors were unable to locate any significant research that elaborates on the mechanical properties of GPC with different cement compositions employing a combination of flyash and GGBS, based on the literature surveyed. However, this research component is crucial to the practical application of environmentally friendly building construction practices. The study has a connection to the building industry's economic growth as well. Therefore, additional research and analysis are needed to create new geopolymers with better mechanical qualities. Sweat is invested in the experimental endeavor to address this significant research gap in order to answer to this call. The fact that few studies have combined these materials is the primary subject of the current work, which looked at the flexural capacity and behaviour of fly ash and GGBS-based one-way slabs reinforced with GFRP rebars. The rebar ratio, slab thickness, and compressive strength were the variables that were being examined. Failure modes, fracture patterns, load-deflection curves, and load-strain curves were all on exhibit. Furthermore, a comparison was made between the experimental data and the predicted flexural strength that was computed using the equations recommended by IS 456-2000 and ACI 440.1R-15 2015.

3. Materials and their properties

3.1. GFRP rebars

GFRP rebars of diameter manufactured by KC CONTECH Chennai (in Colloboration with Composite Group CHELYABINSK, RUSSIA), India. were used as the main flexural reinforcement of slabs. Three samples (G1, G2, and G3) were tested in uni-axial tension using resin-filled steel tubes in the grips to determine the tensile properties, which are displayed in Table 1. The majority of the bars broke free from the grips, indicating the composite's tensile strength.

Table 1.Tensile properties of reinforcements (Experiment)

Specimen ID	Peak Tensile load [kN]	Peak Tensile Extension [mm]	Ultimate Tensile Strength [MPa]	Modulus of elasticity [MPa]	Avg Modulus of elasticity
G1	78.24	15.5	957.99	61651.74	62916.11MPa
G2	78.35	16.2	998.1	61587.5	
G3	78.6	15.3	1001.2	65509.09	
S	78.6	2	520	200000 MPa	

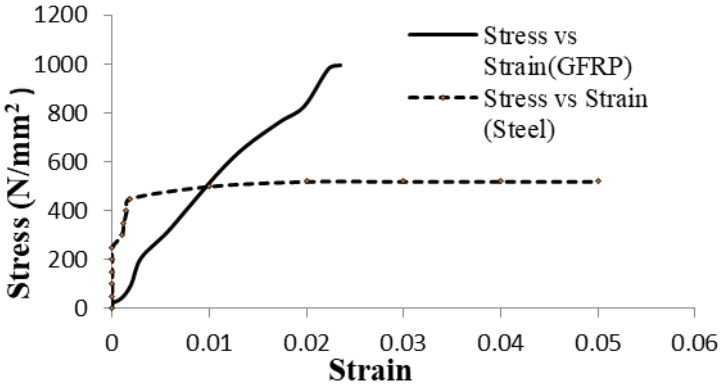

Fig.1.Stress Strain Curve of reinforcements used in the present study

4.GPC Mix Proportion

In this study, M25 and M50 grades of GPC were produced as per IS 10262-2009, the mix design codal provisions. Workability has been examined and three mix proportions of M25 and two mix proportions of M50 have been designed. For two minutes, fly ash, GGBS, and aggregates were mixed in dry condition. The "24-hour old alkaline solution" was then added, and the mixture was stirred for an additional two minutes (Fig. 2 to Fig. 4). Then water and super plasticiser were additionally added within the allowable limit to achieve the desired workability. After the slump test the concrete mixes were poured into the cube moulds (150x150x150 mm) in three layers and electric vibrator was used in each layer to compact the concrete. There are five cubes in every trial. Concrete cubes were cast, allowed to settle for 24 hours, and then left to cure naturally for another 28 days. Tables 2 and 3 show the GPC Mixes mix proportions. Three different mixes for M25 grade and two different mixes for M50 grade have been prepared and tested and the best mix has been selected for the preparation of slabs considering the workability.

Table2. Mix proportions of GPC (M25)

INGREDIENTS	GPC Mixes (M25)		
	M1	M2	M3
Molarity	12	12	12
Flyash	370.494	540	380.29
GGBS	41.17	60	42.25
NAOH	57.63	82.29	54.33
Na_2SiO_3	144.1	205.73	135.8
Fine Agg	773.92	600	709.87
Coarse Agg	1214.40	1200	1267.62

Water	32.178	49.374	32.60
SP	4.12	6	4.23
AAS/Binder	0.49	0.48	0.45
Mix Ratio	**1:1.88:2.95**	**1:1:2**	**1:1.68:3**

Table 3. Mix proportions of GPC (M50)

INGREDIENTS	**GPC Mixes (M50)**	
	M1	**M2**
Molarity	14	14
Flyash	379.04	347.62
GGBS	252.38	283.81
NAOH	30.1	30.1
Na_2SiO_3	134	134
Fine Agg	568.57	568.57
Coarse Agg	1200	1200
Water	23.8	23.8
SP	7.62	7.62
AAS/Binder	0.30	0.30
Mix Ratio	**1:0.9:1.9**	**1:0.9:1.9**

Based on the workability M3 mix (M25) and M2 mix (M50) have been selected and Table 4 depicts the results of the same.

Table 4.Workability and Compressive strength Test Results

S.No	**Mix**	**Mix ratio**	**Workability (Slump ,mm)**	**Compressive Strength,MPa**
1	M25 (GPC)	1:1.68:3(M3:Table.2)	125	38.4
2	M50 (GPC)	1:0.9:1.9(M2:Table.3)	100	60.28

Designing the slab specimens in accordance with IS 456-2000 was done. Four GPC-GFRP slabs and one GPC-Steel slabs made up the experimental program. Table 1 lists the various slab variations. For the purpose of reinforcing all of the slab specimens, 10 mm (Af = 78.5 mm^2) GFRP bars with ultimate tensile strength f_{fu} = 986MPa, modulus of elasticity E_f = 64GPa, and ultimate strain of 2.7% were employed. Every slab is the same length of 2000 mm and width of 600 mm. For every beam, a clear cover of 20 mm was maintained. There were two different slab thicknesses: 100 and 120 mm. The range of the GFRP rebar reinforcing percentage was 0.39 and 0.5%.Two mixes of grades M25 and M50 were included.

Fig.2.Preparation of Alkaline Activator

Fig.3.Preparation of GPC Mix

Fig.4.Ambient curing

5.Flexural Investigations

Four GPC one-way slabs reinforced with GFRP rebars and one GPC one-way slab reinforced with steel rebars made up the trials. Each series included two identical parts (a total of 8 tests) to assure repeatability. Table 5 lists the different parameters taken into account in this investigation along with their corresponding designations. GFRP bars of 10 mm diameter serve as both primary and secondary reinforcements. Two distinct slabs with two different spacings of 280 mm and 187 mm, were constructed. For every slab, there are nine secondary reinforcements arranged at a 180 mm c/c distance. Nylon zip ties are used to tie secondary GFRP reinforcements. For each slab, the bottom cover of the main reinforcements is 20 mm. Rotating mixers were used to assist mix the concrete.Fig.5 to Fig.7illustrate the various phases of the slab construction process.

Table 5. Various Parameters involved in the construction of slabs

Grade of Concrete	Type of Reinforcement	No.of Main Rebars	Thickness of The Slabs	Rebar ratio
M25	Steel	3	100 mm	0.39
M50	GFRP	4	125mm	0.52

Fig.5. Positioning the reinforements

Fig.6.Casting One way slab

Fig.7. Ambient curing of slabs

5.1 Test setup and Instrumentation

Slab specimens are tested using a load frame with a 50-ton capacity. The end conditions of slabs are as follows: one end of the slab rests on a roller support, while the other end rests on a hinge support. Spreader beams are used to facilitate the usage of the two point loading (line loads) system. To prevent local effects, thick rubber or neoprene pads are placed underneath the spreader beams. Spirit levels ensured that the slabs' support end levels were correctly maintained. Static loads are manually imposed using hydraulic jacks with a 250 kN capacity, and load cells or proof rings are used to monitor the stresses. LVDTs, Demec gauges, dial gauges, and surface strain pellets are the tools used to measure the deflections or deformations of the slab.Surface strain gauges on the exterior are pasted to every slab. In order to measure strains using Demec gauges, a standard gauge distance must be established. This is accomplished by pasting brass pellets at the top, bottom, and center fibers at a predetermined distance. In addition to this, mid-span and one-third load locations are monitored for vertical deflections using LVDTs with a range of 0-100 mm. Up until the slabs collapse, the load is gradually imparted in increments of 2 kN. Using a crack width detection microscope, the crack widths are measured on a regular basis. Fig.8 and 9 display the experimental setup.

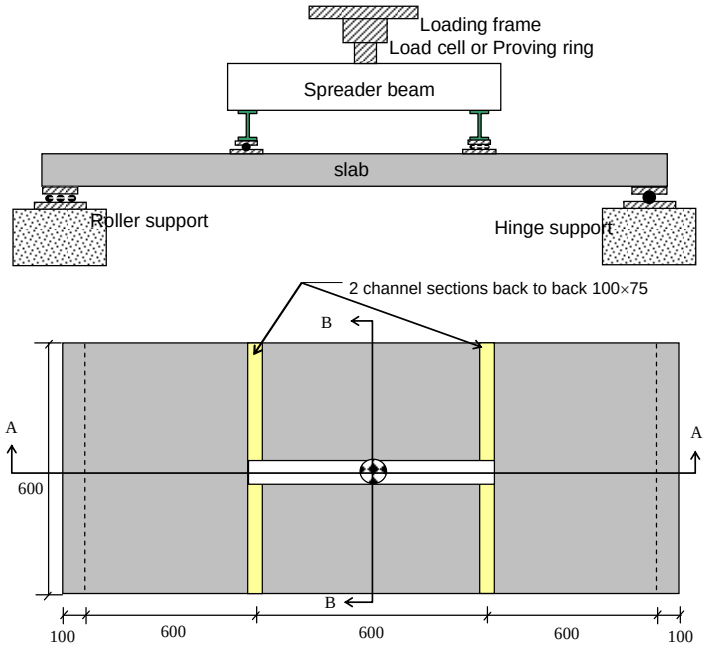

Fig.8. Test Arrangement

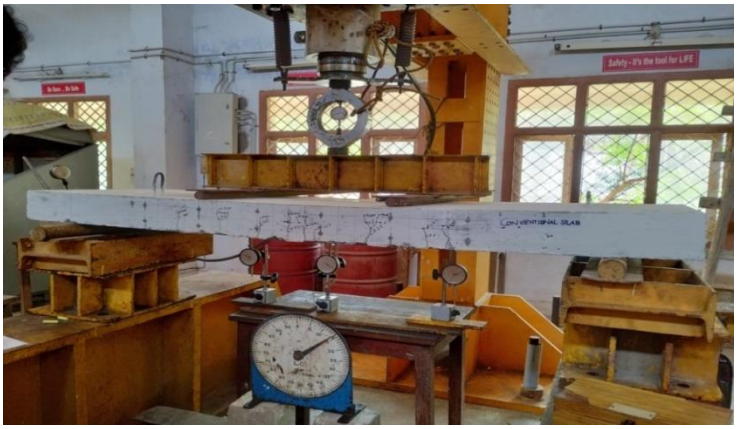

Fig.9.Photograph showing the Experimental Program

6. Experimental Results

The conclusions derived from this static loading test were based on testing 5 one way slabs cast with various factors as mentioned in Table 5 . The description of the five slabs built for this study is provided below the Table 6.

Table 6. Results of Flexural Investigation on Slabs

Sl No	Designation of slabs	P_{fc} (kN)	P_u (kN)	$M_{u,}$ kNm	w_{cr} mm	ΔU mm	ε_c	ε_s
1	GG-M1R1D1	10	40	12	1.7	55	0.0007	0.005
2	GG-M1R2D1	12	47.5	14.25	1.5	60	0.0005	0.0046
3	GG-M1R1D2	15	54	16.2	1.5	39.2	0.0003	0.0046
4	GG-M2R1D1	18	47	14.1	1.2	39.2	0.0005	0.0042
5	GS-M1R1D1	10	36	10.65	0.5	8.5	0.001	0.0054

Where G denotes GPC –GFRP one way slabs; M1-M25 grade of GPC; M2-M50 grade of GPC; R1-0.39% reinforcement ratio; R2-0.5% reinforcement ratio; D1-100 mm thickness slab; D2-120 mm thickness slab; P_{fc}–First Crack Load; P_U –Ultimate Load; M_U –Ultimate Moment; w_{cr}-Crack Width; Δ_U-Ultimate Deflection; ε_s –Strain in steel(ultimate) ;ε_c-Strain in Concrete (ultimate)

6.1.First Crack load and Ultimate Load

In comparison to similar slabs, the increase in reinforcing ratios, concrete grade, and slab thickness showed higher strengths and smaller fracture widths. In comparison to slabs strengthened with traditional reinforcements, those reinforced with GFRP reinforcements have demonstrated superior performance. For GPC slabs strengthened with GFRP reinforcements, the P_U increases by 18.75% and P_{fc} increases by 20% when the reinforcement ratio is increased from 0.39 to 0.52. Similarly,on increasing the slab thickness from 100 mm to 125 mm, P_U increases by 35% and P_{fc} increases by 50% . On increasing the grade of concrete from M25 to M50 for GPC slabs reinforced with GFRP reinforcements, the P_{fc} increases by 80% and P_U increases by 17.5 %. On comparing the GPC slabs reinforced with GFRP reinforcements with GPC slabs reinforced with conventional reinforcements, P_{fc} of GFRP slabs increases by 15% and P_U increases by 12.7 % than that of Steel reinforced slabs.

6.2 Load – Deflection response

For every slab specimen, the load against mid-span deflection curves were displayed from Fig.10 to Fig.13. Initially, the mid-span deflection rose linearly up to a particular load (i.e., the yield load) and then varied non-linearly upto a maximum value as the load increased. In comparison to GPC-Steel slabs, GFRP reinforced slabs exhibit a larger drop in stiffness in the load deflection response caused by static loading. GFRP reinforced slabs show no yielding of reinforcements and the deflection increases with the increase in load, exhibiting some ductility despite the brittle nature of GFRP rebars. While the slabs were being tested under two point static loads, two significant behavioural stages were noted. Given that the beam is still uncracked, a linear branch with a sharp slope and even almost a linear segment was seen till failure when the cracking process began. Every time a crack forms, the load in the slabs changes suddenly. Every slab was intended to fail in the flexure, which was identified by the emergence of cracks in the zone of tensile stress.

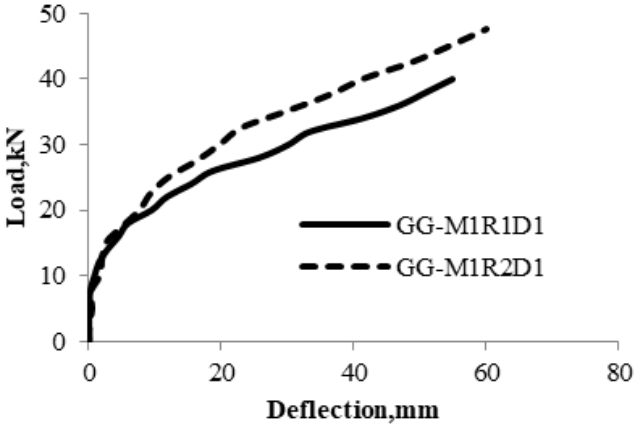

Fig.10.Load versus Deflection (GPC slabs reinforced with two different GFRP reinforcement ratios

Fig.10 shows the ultimate deflection of GG-M1R2D1 was 1.09 times greater than GG-M1R1D1.It has been observed that increase in the tensile reinforcements increases the deflection because the additional tensile (main) reinforcement provides greater resistance to bending and flexural stresses and thus the deflection also slightly increases.

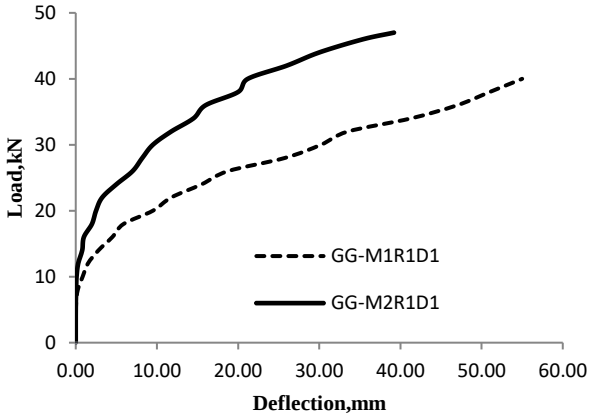

Fig.11.Load deflection response (Slabs with different GPC Concrete strength)

The stiffness of the slab increases and the deflection lowers by 0.7 times when the concrete grade is increased from 25 N/mm^2 to 50 N/mm^2 (Fig.11). This may be due to the well graded higher quantity of concrete or GPC mixture promotes a higher bond strength and minimizes the deflection.

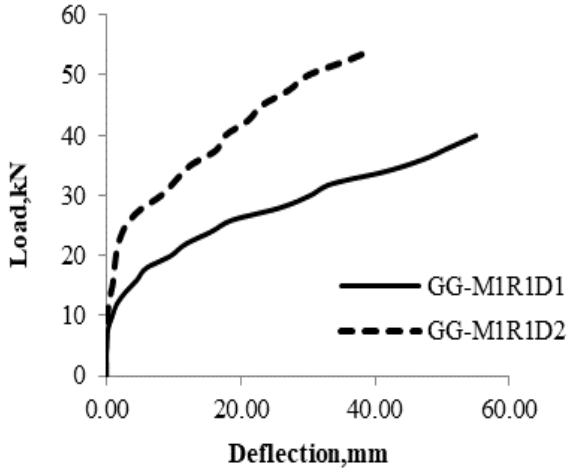

Fig.12.Load-deflection response (GPC-GFRP slabs Varying in thickness)

On increasing the thickness of slabs from 100 mm to 120 mm, the stiffness of the slab increases and the deflection decreases by 0.7 times (Fig.). A thicker slab distributes loads over a larger area, reducing stress and impending failure and more resistant to deflection.

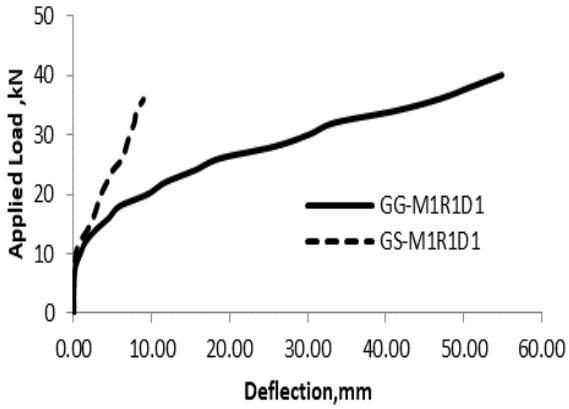

Fig.13.Load deflection response of GPC slabs reinforced with Steel and GFRP Reinforcements

When GFRP rebars and steel-reinforced GPC slabs are compared, the latter's deflection is six times larger than the former's. GFRP slabs have a low elasticity modulus compared to steel, which causes them to deflect and break excessively.

6.3 Strain distribution

The ratio of the length of the modified specimen to its original length is called strain, and it reflects the deformation of the specimen under load. Every specimen received a consistent load, and at different loading phases, the strain along the mid-span was measured. Fig.14 displays the strain distributions along the slab thickness. The GFRP reinforcements in the tension side of the concrete slabs have been found to react similarly to the GFRP reinforcements that are tested in pure tension. Thus, it suggests that, as expected in the design of reinforced concrete, there is a complete link between the reinforcing bars and the concrete. The concrete surface strain in GFRP reinforced slabs is approximately two to three times greater than the conventional slabs under the same load level.. At the initial stages of loading the slabs exhibit same strain values and on further increasing load the strain of various slabs increases whereas at the final stage all the slabs fail at strain level ranges from 0.0029 to 0.005. The tensile strain at ultimate stage of GG-M1R1D1 seems to be 25%, 28.2%, 39% and 72.4 % greater than GS-M1R1D1, GG-M1R2D1, GG-M2R1D1 and GG-M1R1D2 respectively.

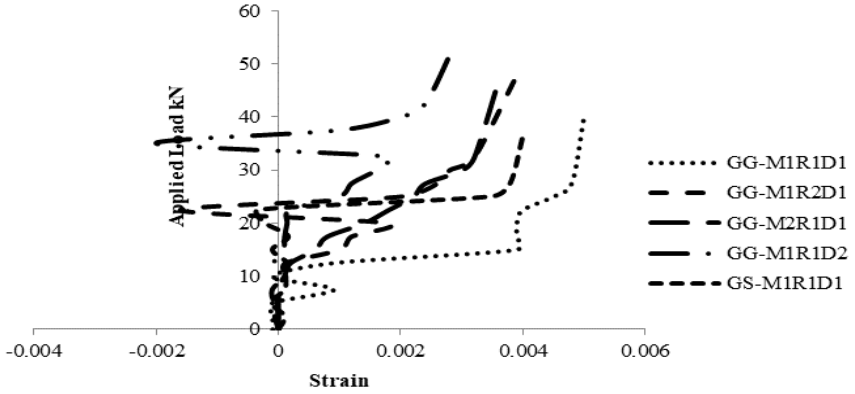

Fig.14. Tensile strain plots of all five slabs

6.4 Crack formations and failure mechanisms

During loading, the beginning and progression of fissures in the slabs were noted and monitored. The length and orientation of them were marked on the slabs immediately during loading (Fig.15 and Fig.16) and the load value and crack widths corresponding to crack initiation were measured. The average value is presented in Table 6. While calculating the cracking load, the beams self-weight was left out. The cracks in all of the slabs began in the pure bending zone and widened as the load rose. When the tensile stresses in concrete surpass the concrete's modulus of rupture, cracks start to show up at the bottom surfaces of the slabs. The slab's middle is the location where the first fracture occurs, and it spreads gently along its breadth. As the load is applied more forcefully while the loading is static, cracks continue to grow. Every slab has some kind of flexural failure. When GFRP reinforced slabs are subjected to their maximum load, the concrete crushes and the GFRP reinforcements tear. Steel reinforced GPC slab exhibit the flexural kind of failure. By raising the thickness, concrete grade, and reinforcing ratio of the slabs, the ultimate load carrying capacity of GFRP reinforced slabs is enhanced and the accompanying deflections with crack size are minimized. Slabs reinforced with GFRP perform better than those reinforced with steel with respect to the ultimate load. This is primarily explained by the fact that concrete and GFRP reinforcements have equal moduli of elasticity values in addition to the GFRP reinforcements' linearly elastic performance.

Fig.15. Crack pattern of GPC-Steel Slab

Fig .16. Crack pattern of GPC-GFRP Slab

7. Theoretical investigations

In order to suggest the development of structure, the notion of limit state design has been introduced. Ultimate load, deflections and crack sizes at service load, were the three most significant limit states. The strategy is becoming more widely accepted. Therefore, elastic theory is only employed to ensure serviceability; ultimate strength theory is increasingly being used to proportion sections. It is well known that the optimal design strategy for reinforced concrete should include the best aspects of working stress design and ultimate strength. This is preferred because, even with an appropriate load factor, there is a risk of excessive deflections at service loads if sections are designed using ultimate strength provisions alone. If the bars are unevenly spaced or the steel tensions are higher, there could be excessive cracking. Therefore, in order to guarantee a suitable design, it is necessary to verify that the crack widths and deflections during service loads fall within acceptable limiting values, which are determined by the structure's functional requirements. Elastic theory must be used for this check.

7.1.Moment of Resistance

For $\rho_{GFRP} \leq \rho_{B-GFRP}$, FRP rupture failure mode governs, and the expression for ultimate moment of resistance of under reinforced condition are given in (1).

$$M_{uR} = \left(f_{GFRPu} \frac{\rho_{GFRP}}{100} \left[1 - \beta_1 \frac{f_{GFRPu}}{f_{cu}} \frac{\rho_{GFRP}}{100} \right] \right) bd^2$$

(1) For $\rho_{GFRP} \geq \rho_{B-GFRP}$, crushing of the concrete occurs. Based on the compatibility conditions the following Equation (2) resulted.

$$f_{GFRP} = \left(\sqrt{\frac{(E_{GFRP}\varepsilon_{cu})^2}{4} + \frac{\alpha f_{cu}}{\rho_{GFRP}} E_{GFRP}\varepsilon_{cu}} \right) - 0.5E_{GFRP}\ \varepsilon_{cu} \quad (2)$$

Where f_{GFRP} s the GFRP reinforcement's ultimate stress in tension. The ultimate moment of resistance expression for over reinforced rectangular section is given in (3).

$$M_{uR} = \left(f_{GFRP} \frac{\rho_{GFRP}}{100} \left[1 - \beta_1 \frac{f_{GFRP}}{f_{cu}} \frac{\rho_{GFRP}}{100} \right] \right) bd^2 \quad (3)$$

7.2 Deflection

Using basic structural analysis techniques, expressions for the maximum elastic deflection of a homogeneous slab with an effective span of L and flexural rigidity $E_c I_{exp}$ (for any loading and support conditions) can be generated for two point loads. The formula for maximum deflection, ignoring the shear component of deflection, is shown in (4).

$$\delta_{\max} = k_m \frac{Ml^2}{E_c I_{\exp}} \quad \text{or}$$

$$\delta_{\max} = k_m \psi_{\max} l^2 \tag{4}$$

where k_m is a constant and this varies according to the flexural rigidity EI, end restraint circumstances, and load distribution. For section with two point loading under simply supported slab conditions, k_m = 0.15(for GFRP) and 0.1(for Steel) (Based on Experiment); L= clear span; $\psi_{\max} = \frac{\varepsilon_{cu} + \varepsilon_{GFRP}}{d}$ = curvature at ultimate stage (Based on Experiment) ; I_{exp} = experimental moment of inertia (mm^4); P = applied load in kN; E_c = modulus of elasticity of concrete, MPa = 5000 $\sqrt{f_{ck}}$ .L=length of slab (Support to support); a=Shear span; E_{GPC}=Modulus of elasticity of GPC and δ_{exp}=Experimental deflection

7.3Effective Second Moment of Area for GFRP Reinforced Sections

Numerous empirical formulae have been put out and included in various concrete design standards for the computation of the effective second moment of area, or I_{eff} (for determining short-term deflections). While some of these formulations (which incorporate stress-strain relations and force equilibrium) are based on moment-curvature associations, others are based on strain/stress changeover in the area among cracks. The expression for I_{eff} in this study is derived from Branson's equation (Branson 1977) and has the following form(5).

$$I_{eff} = \left(\frac{M_{cr}}{M}\right)^3 I_{gr} + \left[1 - \left(\frac{M_{cr}}{M}\right)^3\right] I_{cr}$$

for $M > M_{cr}$

(5)

There is a fair amount of agreement between the experimental and theoretical values of deflections when using this expression, which is straightforward and simpler to compare with test findings. For GFRP reinforced concrete slabs, the stiff response is provided by I_{eff} in Branson's equation. The deflections of GFRP reinforced GPC slabs upon load application are estimated by the current deflection equations. I_g (Gross Moment of Inertia), is given below (6).

$$I_g = \frac{bD^3}{12} \tag{6}$$

Similar to regular steel-reinforced concrete, the transformed or cracked second moment of area is expressed as (7)

$$I_{cr} = \frac{bx_u^3}{3} + \eta_{GFRP} A_{GFRP} (d - x_u)^2 \tag{7}$$

$$\eta_{GFRP} = \frac{E_{GFRP}}{E_{GPC}} \tag{8}$$

where η_{GFRP} =Modular ratio for the GFRP reinforcement (8)and x_u =section's neutral axis depth under service load.

8. Flexural Cracking

Reducing the average crack width is the main goal of crack control. This is necessary for durability, especially in harsh environmental circumstances, but it's also necessary for aesthetic reasons. Many variables (bond strength, the depth of the member, tensile strength , the diameter, spacing of longitudinal rebars and thickness of the concrete cover) which are connected to one another, affect the crack widths in flexural members.. Because of the poor tension capacity and low failure strain (in tension) of GPC, flexural tensile cracks cannot be completely removed. Because the strains created in GFRP reinforcements at service load levels are substantially larger, this is especially true when using GFRP reinforcing bars. While flexural cracking is unavoidable, it is preferable to have many evenly spaced, tiny hairline fractures as opposed to a few, larger fissures. Because of the intrinsic randomness in the width and spacing of fractures, concrete cracking cannot be accurately predicted. The techniques used to calculate fracture widths merely make an effort to forecast the most likely maximum crack width seen in laboratory experiments.

The problem of estimating the maximum probable width of surface cracks in a flexural slab system is quite complex. Over the course of the last forty years, there has been significant research in this area, and various equations have been developed to predict crack widths, some of which differ

significantly from one another. Different international codes use different approaches (with semi-empirical formulae). After comparing the current experimental test findings with the predictions of the most popular international codal methods, it was determined that the Gergely and Lutz formulation, which slightly modified the bond related coefficient, was appropriate for the investigation. Therefore, the well-known Gergely-Lutz formula (9) is used in this study to offer the likely crack width expressions.

$$w_{cr} = k_g f_{GFRP} \frac{h_2}{h_1} k_b \sqrt[3]{d_c A} \quad (9)$$

Where $k_g = \frac{2}{E_{GFRP}}$ = is a material-dependent coefficient; $h_2 = D - kd; h_1 = d - kd; d_c =$ the thickness of the concrete cover measured from the extreme tension fiber to the center of the closest bar; $f_{GFRP} =$ stress at the centroid of the rebar in tension ;; *d*= depth of neutral axis; *D*=overall depth of the slab; $A = \frac{A_e}{n} = \frac{2(D-d)b}{n}$;

$n =$ number of bars in tension; $b =$ breadth of the slab; k_b = bond related coefficient, which is taken as 1.25 for GFRP bars and 1.0 for steel bars, infers that GFRP bars have a different bond behavior than that of steel bars (ACI 440R-96 1996). For GPC slabs reinforced with GFRP and Steel reinforcements, the actual and theoretical values of load, deflection, and crack width are provided in Table 7.

Table 7. Load, Deflection and Crack width obtained from Experimental and Theoretical results(Comparison)

SL NO	Designation of slabs	Experimental values		Theoretical values		W_{cr} mm		Ultimate Deflection, mm	
						Exp	Theo		
		P_u (kN)	P_{fc} (kN)	P_u (kN)	P_{fc} (kN)			Exp	Theo
1	GG-M1R1D1	40	12	38.52	11.67	1.35	1.41	55	50.66
2	GG-M1R2D1	47.5	15	45.44	11.67	1.3	1.35	60	54.94
3	GG-M1R1D2	54	20	51.32	16.8	1.2	1.29	39.2	37.9
4	GG-M2R1D1	47	18	44.5	16.5	1.0	1.26	39.2	31.88
5	OS-M1R1D1	36	8	29.92	11.67	0.35	0.21	8.45	7.54
6	OG-M1R1D1	38.6	10	38.52	11.67	1.43	1.41	58.25	50.82
7	GS-M1R1D1	35.5	10	29.92	11.67	0.32	0.21	8.5	7.49

9. Conclusions

Below is a summary of the experimental and Theoretical study's findings using the five distinct parametric one-way GPC slabs:

- The mix design used to prepare GPC Mix is same that of OPC and based on workability a better mix proportion has been selected and used in the current study for both M25 and M50 mixes.
- On increasing the rebar ratio, thickness of the slabs, grade of GPC the ultimate load increases and corresponding deflection decreases.
- Reinforcing GPC with steel rebar decreases the deflection.
- The concrete surface strain in GFRP reinforced GPC slabs is 25 % lesser than Steel reinforced GPC slabs.
- The failure strain of GPC slab varies significantly within the range of 0.003 – 0.005.
- Moment capacity equations are modified for the FRP rupture and concrete crushing failure modes by comparing the FRP reinforcement ratio, ρ_{GFRP} to the balanced reinforcement ratio, ρ_{B-GFRP} .
- Branson equation is suggested for deflection expression based on the experimental study. Gergely-Lutz formula is used for the calculation

of crack width for the GFRP reinforced one-way concrete slabs with suitable modification .

- The crack patterns and failure observed for GPC slabs failed initially by yielding or rupture of rebars accompanied with crushing of concrete.

Acknowledgement

Our Sincere thanks to KC CONTECH Chennai, Mettur Thermal Power Station, Tamil Nadu and Navoday Science Pvt. Ltd,Chennai for having provided GFRP rebars, Fly Ash and GGBS respectively.

References

[1] Abraham, R., Raj, S., & Abraham, V. (2013). Strength and behaviour of geopolymer concrete beams. International Journal of Innovative Research in Science, Engineering and Technology, 2(1), 159–166.

[2] ACI 440.1R-15. (2015). Guide for the design and construction of Concrete Reinforced with Fiber Reinforced Polymers (FRP) bars, ACI Committee 440. Farmington Hills, MI, USA: American Concrete Institute.

[3] Ascione, L., Mancusi, G., & Spadea, S. (2010). Flexural behaviour of concrete beams reinforced with GFRP bars. Strain, 46(5), 460–469. https://doi.org/1 0.1111/j.1475-1305.2009.00662.x

Ashveenkumar P., Preethi M., Prashanth P. 2021. Mechanical properties of geopolymer concrete with varying cement content using flyash and ground granulated blast furnace slag. International Journal of Engineering, Science and Technology, Vol. 13, No. 4, pp. 57-64. doi: 10.4314/ijest.v13i4.7

[4] Bischoff PH, Ospina C, Alkhrdaji T,(2009). Serviceability of concrete members reinforced with internal/external FRP reinforcement. Farmington Hills, MI: American Concrete Institute; 2009. p. 53-76.

[5] Cui Y., Gao K., and Zhang P. 2020, Experimental and statistical study on mechanical characteristics of geopolymer concrete, Materials (Basel), Vol. 13, No. 7, Article 1651. doi: 10.3390/ma13071651

[6] Hemn Qader Ahmed, Dilshad Kakasor Jaf, Sinan Abdulkhaleq Yaseen (2020) Flexural strength and failure of geopolymer concrete beams reinforced with carbon fibre-reinforced polymer bars Construction and Building Materials Volume 231, 20 January 2020, 117185

Kara IF, Ashour AF. Flexural performance of FRP reinforced concrete beams. Composite Structures. 2012;94:1616-25.

[7] Kathirvel P., Saravanarajamohan K., Shobana S., Bhaskar A. 2013, Effect of replacement of slag on the mechanical properties of flyash based geopolymer concrete, International Journal of Engineering and Technology, Vol. 5, No. 3, pp. 2555-2559

[8] Kumar A.C.S., Muthu K.U., Sagar S.A., Yadav D.T., 2018, Experimental investigation of mechanical properties of geo polymer concrete with GGBS and hybrid fibers, International Journal of Applied Engineering Research, Vol.13, No. 7, pp. 292-298

[9] Ling Y., 2018, Proportion and performance evaluation of fly ash based geopolymer and its application in engineered composites, Ph.D. thesis, Department of Civil, Construction, and Environmental Engineering, Iowa State University, USA.https://doi.org/10.31274/etd-180810-6028

[10] G.B. Maranan1, A.C. Manalo1,*, B. Benmokrane2, W. Karunasena1, and P. Mendis3Evaluation of the flexural strength and serviceability of geopolymer concrete beams reinforced with Glass-Fibre-Reinforced Polymer (GFRP) Engineering Structures · October 2015 DOI: 10.1016/j.engstruct.2015.08.003

[11] Masmoudi R, Benmokrane B, Chaallal O. Cracking behaviour of concrete beams reinforced with FRP bars. Canadian Journal of Civil Engineering. 1996;23:1172-9

[12] Naidu P.G., Prasad A.S.S.N., Adiseshu S., Satayanarayana P.V.V., 2012, A study on strengthproperties of geopolymer concretewith addition of GGBS, International Journal of EngineeringResearch and Development, Vol. 2, No. 4, pp. 19-28.

[13] Patel M., Rao P.S. and Patel T.N., 2013, Experimental investigation on strength of high performance concrete with GGBS and

crusher sand, Indian Journal of Research, Vol. 3, No. 4, pp. 114-116

[14] Rajamane N. P., Lakshmanan N. and Nataraja M.C., 2009, Geopolymer concrete - a new eco-friendly material of construction,NBM & CW, Infra Construction and Equipment Magazine, India

[15] Ralli Z.G. and Pantazopoulou S.J., 2021, State of the art on geopolymer concrete, International Journal of Structural Integrity,Vol. 12 No. 4, pp. 511-533. https://doi.org/10.1108/IJSI-05-2020-0050

[16] SaiKumar.A and G.Kumaran(2021), "Performance of Geopolymer Concrete Reinforced with FRP Rebars-A Review" Revista GEINTEC-Gestao Inovacao E Tecnologias ,ISSN:2237-0722,Vol.11(3),May2021,pp 388-394

[17] SaiKumar.A and G.Kumaran(2021), "Mix Design of Geopolymer concrete-A review",Adalya Journal,[Web of science]Impact Factor-5.3 ISSN-1301-2746,Vol9(8),Aug 2021,pp182-188

[18] Supraja V. and Rao M.K., 2016, Experimental study on geopolymer concrete incorporating GGBS, International Journal of Electronics, Communication & Soft Computing Science and Engineering, Vol. 2, No. 2, pp. 11-15 The Concrete Conundrum, 2022, https://www.rsc.org/images/Construction_tcm18-114530.pdf